

Electrostatic Properties of Adsorbed Polar Molecules: Opposite Behavior of a Single Molecule and a Molecular Monolayer

Dudi Deutsch,^{†,‡} Amir Natan,[†] Yoram Shapira,[‡] and Leeor Kronik^{*,†}

Contribution from the Department of Materials and Interfaces, Weizmann Institute of Science, Rehovoth 76100, Israel, and Department of Physical Electronics, Tel Aviv University, Tel Aviv 69978, Israel

Received November 23, 2006; E-mail: leeor.kronik@weizmann.ac.il

Abstract: We compare the electrostatic behavior of a single polar molecule adsorbed on a solid substrate with that of an adsorbed polar monolayer. This is accomplished by comparing first principles calculations obtained within a cluster model and a periodic slab model, using benzene derivatives on the Si(111) surface as a representative test case. We find that the two models offer diametrically opposite descriptions of the surface electrostatic phenomena. Slab electrostatics is dominated by *dipole reduction* due to intermolecular dipole–dipole interactions that partially depolarize the molecules, with charge migration to the substrate playing a negligible role due to electric field suppression outside the monolayer. Conversely, cluster electrostatics is dominated by *dipole enhancement* due to charge migration to/from the substrate, with only a small polarization of the molecule. This establishes the important role played by long-range interactions, in addition to local chemical properties, in tailoring surface chemistry via polar molecule adsorption.

Introduction

Adsorption of (typically organic) molecules on inorganic substrates is an intriguing approach for controlling and tuning surface and interface electronic properties (see, e.g., refs 1–13). Most experimental work aimed at understanding, developing, and applying this approach has dealt with molecular *monolayers* adsorbed on periodic surfaces. The electronic structure of a *single* molecule adsorbed on a periodic surface has been investigated mostly by examining the current–voltage charac-

teristics through a single molecule, using scanning tunneling spectroscopy.^{14,15}

A tacit assumption in most chemical analyses is that the local chemical environment controls the chemical bonding and ergo all other properties of the system. This can be viewed as a special case of Kohn’s “near-sightedness principle” of quantum mechanics.¹⁶ According to this principle, perturbation of the external potential at a distant region from a given location has a small effect on any static property of a many-particle system at that location. “Near-sightedness” is well-reflected in the two most common approaches to atomistic modeling of an adsorbed monolayer. One approach employs a periodic *slab* model (refs 17–23 are some recent examples), where a “super cell” with the true two-dimensional surface geometry is constructed, with a finite number of layers modeling the inorganic substrate.²⁴ However, a *cluster* model, where a single molecule is adsorbed

[†] Weizmann Institute of Science.

[‡] Tel Aviv University.

- (1) Vilan, A.; Shanzler, A.; Cahen, D. *Nature (London)* **2000**, *404*, 166. Ashkenasy, G.; Cahen, D.; Cohen, R.; Shanzler, A.; Vilan, A. *Acc. Chem. Res.* **2002**, *35*, 121.
- (2) Cohen, R.; Kronik, L.; Shanzler, A.; Cahen, D.; Liu, A.; Rosenwaks, Y.; Lorenz, J. K.; Ellis, A. B. *J. Am. Chem. Soc.* **1999**, *121*, 10545. Cohen, R.; Kronik, L.; Vilan, A.; Shanzler, A.; Rosenwaks, Y.; Cahen, D. *Adv. Mater.* **2000**, *12*, 33.
- (3) Zuppiroli, L.; Si-Ahmed, L.; Kamaras, K.; Nüsch, F.; Bussac, M. N.; Ades, D.; Siove, A.; Moons, E.; Grätzel, M. *Eur. Phys. J. B* **1999**, *11*, 505. Krüger, J.; Bach, U.; Grätzel, M. *Adv. Mater.* **2000**, *12*, 447.
- (4) Crispin, X.; Geskin, V.; Crispin, A.; Cornil, J.; Lazzaroni, R.; Salaneck, W. R.; Bredas, J. L. *J. Am. Chem. Soc.* **2002**, *124*, 8131.
- (5) Seki, K.; Hayashi, N.; Oji, H.; Ito, E.; Ouchi, Y.; Ishii, H. *Thin Solid Films* **2001**, *393*, 298.
- (6) Ishii, H.; Sugiyama, K.; Ito, E.; Seki, K. *Adv. Mater.* **1999**, *11*, 605.
- (7) Boulas, C.; Davidovits, J. V.; Rondelez, F.; Vuillaume, D. *Phys. Rev. Lett.* **1996**, *76*, 4797.
- (8) Park, S.; Kampen, T. U.; Zahn, R. T.; Braun, W. *Appl. Phys. Lett.* **2001**, *79*, 4124.
- (9) Hartig, P.; Dittrich, T.; Rappich, J. *J. Electroanal. Chem.* **1997**, *524–525*, 120.
- (10) de Villeneuve, H.; Pinson, J.; Bernard, M. C.; Allongue, P. *J. Phys. Chem. B* **1997**, *101*, 2415.
- (11) Saito, N.; Hayashi, K.; Sugimura, H.; Takai, O. *Langmuir* **2003**, *19*, 10632.
- (12) Linford, M. R.; Fenter, P.; Eisenberger, P. M.; Chidsey, C. E. D. *J. Am. Chem. Soc.* **1995**, *117*, 3145.
- (13) Haick, H.; Ambrico, M.; Ligonzo, T.; Tung, R. T.; Cahen, D. *J. Am. Chem. Soc.* **2006**, *128*, 6854.

- (14) Guisinger, N. P.; Yoder, N. L.; Hersam, M. C. *Proc. Natl. Acad. Sci. U.S.A.* **2005**, *102*, 8838.
- (15) Guisinger, N. P.; Greene, M. E.; Basu, R.; Baluche, A. S.; Hersam, M. C. *Nano Lett.* **2004**, *4*, 55.
- (16) Kohn, W. *Phys. Rev. Lett.* **1996**, *76*, 3168. Prodan, E.; Kohn, W. *Proc. Natl. Acad. Sci. U.S.A.* **2005**, *102*, 11635.
- (17) Schmidt, W. G.; Seino, K.; Preus, M.; Hermann, A.; Ortmann, F.; Bechstedt, F. *Appl. Phys. A* **2006**, *85*, 387.
- (18) Yanagisawa, S.; Morikawa, Y. *Chem. Phys. Lett.* **2006**, *420*, 523.
- (19) Perebeinos, V.; Newton, M. *Chem. Phys.* **2005**, *319*, 159.
- (20) Segev, L.; Salomon, A.; Natan, A.; Cahen, D.; Kronik, L.; Amy, F.; Chan, C. K.; Kahn, A. *Phys. Rev. B* **2006**, *74*, 165323.
- (21) Heimel, G.; Romaner, L.; Bredas, J. L.; Zojer, E. *Phys. Rev. Lett.* **2006**, *96*, 196806.
- (22) Sun, Q.; Selloni, A. *J. Phys. Chem. A* **2006**, *110*, 11396.
- (23) Rusu, P. C.; Brocks, G. *Phys. Rev. B* **2006**, *74*, 073414. *J. Phys. Chem. B* **2006**, *110*, 22628.
- (24) Srivastava, G. P. *Theoretical Modelling of Semiconductor Surfaces: Microscopic Studies of Electrons and Phonons*; World Scientific: Singapore, 1999. Srivastava, G. P. *Rep. Prog. Phys.* **1997**, *60*, 561.

on a finite-sized cluster is also often employed (see, e.g., refs 25–29). While such a model appears to be more suitable for modeling a single molecule on a surface, its use for monolayers is easily justified within “near-sightedness” if the cluster adequately represents the local chemical environment of the molecule.

The minimum cluster size needed for sufficiently accurate predictions naturally depends significantly on both the investigated property and the specifics of the modeled system.^{27,28} Nevertheless, systematic comparisons between slab and cluster calculations do indeed confirm that good agreement between the two can be obtained^{25,28,30} and agreement between cluster model calculations and monolayer experimental results has been convincingly demonstrated for some systems.³¹ This is important, because using cluster models in lieu of slab ones often holds a practical advantage when performing first principles calculations based on density functional theory (DFT).³² Calculations of molecules within DFT are often performed with hybrid functionals.³³ Slab calculations are often (though not always) performed with a plane-wave basis set, for which the evaluation of the exchange integrals inherent in hybrid functional calculations is numerically inconvenient. Conversely, cluster model calculations are usually based on Gaussian basis sets, for which the exact exchange integrals are evaluated analytically.

An important special case of tuning substrate properties with adsorbed molecules involves adsorbed *polar molecules*. These are often used to modify work functions and barrier height values (see, e.g., refs 1, 3, 4, 13). Furthermore, changes in the dipole of the adsorbed molecules are often invoked as the controlling factor in novel chemical and biological molecule-based sensing electronic devices.^{34–38} However, the equivalence of an adsorbed monolayer and a single adsorbed molecule is then no longer obvious.^{36,39} This is because, in polar molecules, inherently long-ranged electrostatic forces may play a major role, resulting in fundamental physical and ergo chemical differences between an adsorbed monolayer and an adsorbed single molecule, even in the absence of any modification of the “local” chemistry.

In this article, we systematically examine the similarities and differences in the electrostatic properties of a single adsorbed *polar* molecule and an adsorbed *polar* monolayer. This is achieved by using DFT to compute the electrostatic properties of benzene derivatives with strongly varying dipole moments, both for a single molecule adsorbed on model silicon clusters

of varying size and for molecular monolayers. We find striking *qualitative* differences between the two approaches: Slab electrostatics is dominated by *dipole reduction* due to electronic polarization of the molecules, with charge migration to the substrate playing a negligible role. Conversely, cluster electrostatics is dominated by *dipole enhancement* due to charge migration to the substrate, with only a small polarization of the molecule. This establishes the important role played by *coverage*, in addition to local chemical properties, in tailoring surface chemistry via polar molecule adsorption.

Computational Details

Density functional theory (DFT), as implemented in the Gaussian 03 software suite,⁴⁰ was used for all the calculations. We solved the Kohn–Sham equations within the local density approximation (LDA), as parametrized by Vosko et al.⁴¹ We have chosen LDA because of its well-known ability to describe both Si and benzene very well and also for ease of comparison with previously reported periodic slab calculations.³⁹ We note that LDA is well-known to overestimate charge transfer in polarized systems⁴² and may overestimate the substrate response to an adsorbed dipole. However, this does not hinder the prediction and rationalization of the large qualitative differences between single molecule and monolayer calculations that are presented below.

All calculations were performed with the 6-31++G(3df,2pd) basis set, where the Pople 6-31G all electron basis set⁴³ is supplemented by extra polarization⁴⁴ and diffuse⁴⁵ functions on hydrogen and heavy atoms. These functions are well-known to be necessary for a reliable description of the charge density for highly polar molecules. Careful convergence tests have found that this basis set is sufficient for all calculations presented below. For strict convergence, all self-consistent calculations were performed with a “tight” threshold criterion⁴⁰ and all integration grids were chosen to be “ultrafine.”⁴⁰

Three different-sized clusters were built as models of the Si(111) surface, as shown in Figure 1. The “small” cluster has only a single silicon atom (capped by three hydrogen atoms), whereas the “medium” and “large” clusters contain 14 and 38 silicon atoms, respectively, with hydrogen passivation of all silicon dangling bonds. The “medium” and “large” clusters both contain six silicon layers but differ from each other in the *xy* plane.

On each cluster, four different benzene derivatives were adsorbed vertically: benzene, aniline, chlorobenzene, and nitrobenzene. These molecules differ from each other significantly in the *z* component of their dipole moment. The molecules were first optimized geometrically in their gas phase. They were then “grafted” on the clusters, where for the “medium” and “large” clusters an initial geometry of the Si(111) surface was assumed, with the detailed geometry and the substrate–molecule Si–C bond length taken from previous geometry optimizations performed within a slab model.³⁹ The whole system, comprised of cluster and adsorbed molecules, was subsequently optimized geometrically. Default convergence criteria were used for the gas-phase molecules and the molecule on “small” cluster configurations. For numerical expediency, the “loose” criterion was used for molecules on the “medium” and “large” cluster configurations.⁴⁶ Partial dipole

(25) Steckel, J. A.; Phung, T.; Jordan, K. D. *J. Phys. Chem. B* **2001**, *105*, 4031.

(26) Iozzi, M. F.; Cossi, M. *J. Phys. Chem. B* **2005**, *109*, 15383.

(27) Halls, M. D.; Raghavachari, K. *J. Phys. Chem.* **2004**, *108*, 2982.

(28) Penev, E.; Kratzer, P.; Scheffler, M. *J. Chem. Phys.* **1999**, *110*, 3986.

(29) Wang, G. T.; Mui, C.; Musgrave, C. B.; Bent, S. F. *J. Am. Chem. Soc.* **2002**, *124*, 8990. Konôpka, M.; Rousseau, R.; Stîch, I.; Marx, D. *J. Am. Chem. Soc.* **2004**, *126*, 12103.

(30) Orlando, R.; Azavant, P.; Towler, M. D.; Dovesi, R.; Roetti, C. *J. Phys.: Condens. Matter* **1996**, *8*, 1123.

(31) Wang, G. C.; Ling, J.; Morikawa, Y.; Nakamura, J.; Cai, Z. S.; Pan, Y. M.; Zhao, X. Z. *Surf. Sci.* **2004**, *570*, 205.

(32) Hohenberg, P.; Kohn, W. *Phys. Rev.* **1964**, *136*, B864. Kohn, W.; Sham, L. J. *Phys. Rev.* **1965**, *140*, A1133.

(33) Becke, A. D. *J. Chem. Phys.* **1993**, *98*, 5648.

(34) Wu, D. G.; Ashkenasy, G.; Shvarts, D.; Ussyshkin, R. V.; Naaman, R.; Shanzer, A.; Cahen, D. *Angew. Chem., Int. Ed.* **2000**, *39*, 4496.

(35) Wu, D. G.; Cahen, D.; Graf, P.; Naaman, R.; Nitzan, A.; Shvarts, D. *Chem.—Eur. J.* **2001**, *7*, 1743.

(36) Cahen, D.; Naaman, R.; Vager, Z. *Adv. Funct. Mater.* **2005**, *15*, 1571.

(37) Patolsky F.; Zheng, G. F.; Lieber, C. M. *Anal. Chem.* **2006**, *78*, 4260 and references therein.

(38) Niwa, D.; Yamada, Y.; Homma, T.; Osaka, T. *J. Phys. Chem. B* **2004**, *108*, 3240.

(39) Natan, A.; Zidon, Y.; Shapira, Y.; Kronik, L. *Phys. Rev. B* **2006**, *73*, 193310.

(40) Frisch, M. J., et al. *Gaussian 03*, revision C.01wis2 (WIS customized version 2); Gaussian, Inc.: Wallingford, CT, 2004.

(41) Vosko, S. H.; Wilk, L.; Nusair, M. *Can. J. Phys.* **1980**, *58*, 1200.

(42) For example, see: Kümmel, S.; Kronik, L.; Perdew, J. P. *Phys. Rev. Lett.* **2004**, *93*, 213002. Dreuw, A.; Head-Gordon, M. *J. Am. Chem. Soc.* **2004**, *126*, 4007.

(43) Hariharan, P. C.; Pople, J. A. *Theor. Chim. Acta* **1973**, *28*, 213.

(44) Dunning, T. H., Jr. *J. Chem. Phys.* **1989**, *90*, 1007.

(45) Petersson, G. A.; Al-Laham, M. A. *J. Chem. Phys.* **1991**, *94*, 6081.

(46) All structures were relaxed to a maximum force smaller than 5×10^{-4} Hartree/Bohr and an RMS force smaller than 4×10^{-5} Hartree/Bohr. Gas-phase molecules and “small” clusters were relaxed to an RMS displacement smaller than 6×10^{-4} Bohr and a maximal displacement smaller than 2×10^{-3} Bohr, while the RMS and maximal displacement for the “medium” and “large” clusters were 2×10^{-3} and 2×10^{-2} Bohr, respectively.

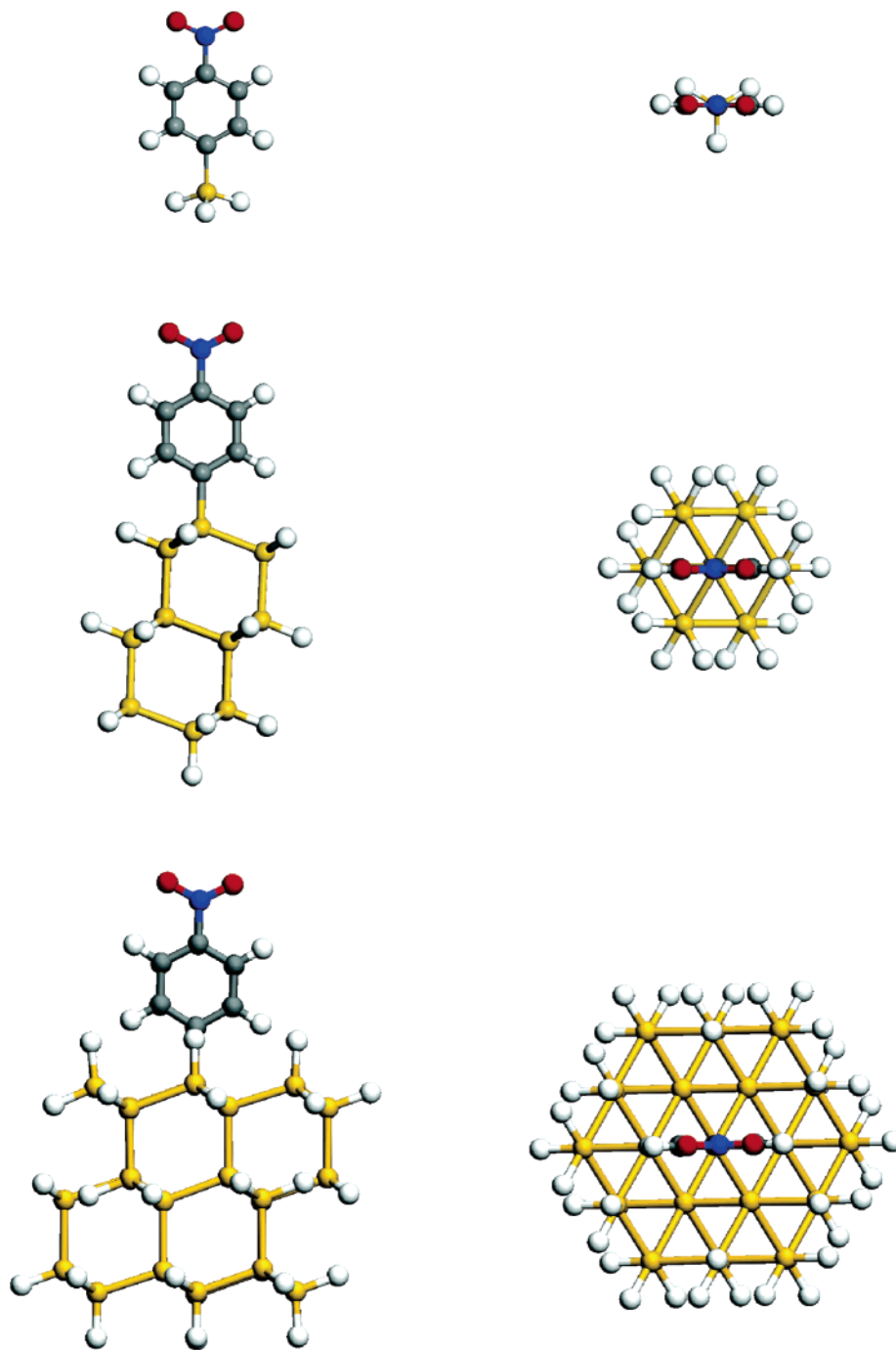


Figure 1. “Ball and stick” models of nitrobenzene on a “small” (top), “medium” (middle), and “large” (bottom) cluster. Left column: Side view. Right column: Top view.

moment⁴⁷ and charge reorganization calculations were performed using the ground state valence electron charge density, calculated using the “Cubgen” utility⁴⁰ of Gaussian03, with a very fine grid of 24 points per Bohr.

Additionally, calculations for an array of molecules that are periodic in the xy plane were performed using the same atomic basis set as that above with periodic boundary conditions.⁴⁸ This was done to guarantee that differences between the results presented below and previous plane wave slab calculations reflect true physical differences and not numerical errors arising from the different choice of basis sets. For each benzene derivative, two “free-standing” arrays of molecules were

built. These correspond to a full (1ML) and partial (0.5ML) coverage, but with the Si substrate *removed* and H replacing Si for the C atom bonded to the Si. The Brillouin zone along the monolayer plane was sampled by an array of 16×10 or 8×10 k-points in the x and y directions for the 1ML and 0.5ML cases, respectively. The molecular positions for these “free-standing” monolayers were taken from previous plane wave calculations³⁹ with no further optimization.

Results and Discussion

1. Dipole Moment, Charge Migration, and Molecular Orbitals in the Cluster Model. To compare the dipolar properties of the gas-phase and cluster-adsorbed molecules, static dipoles along the z -axis were computed for both cases with all

(47) Natan, A.; Kronik, L.; Shapira, Y. *Appl. Surf. Sci.* **2006**, *252*, 7608.

(48) Kudin, K. N.; Scuseria, J. E. *Phys. Rev. B* **2002**, *61*, 16440.

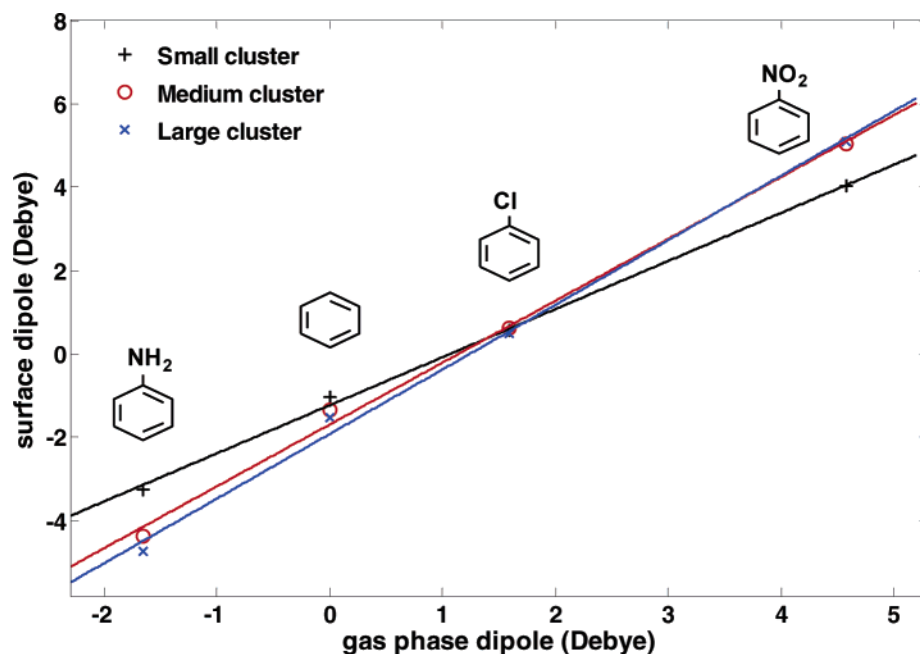


Figure 2. Total dipole moment for the three molecule-adsorbed Si(111) clusters of Figure 1, as a function of gas-phase molecular dipole.

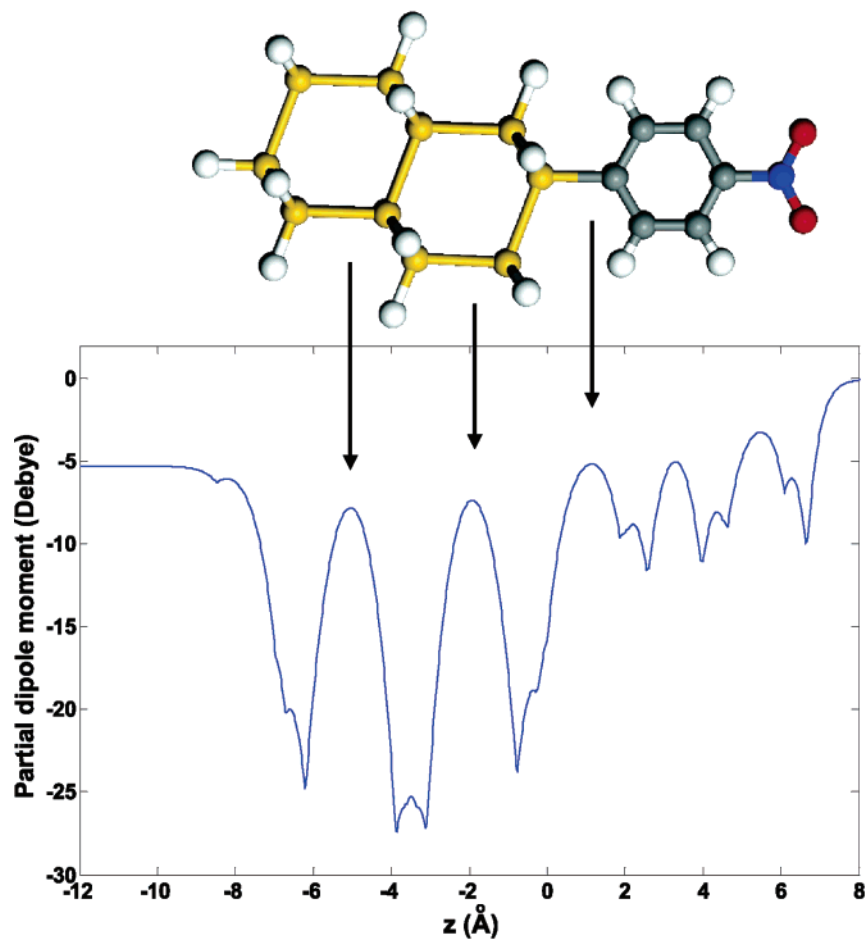


Figure 3. Vertical component of the partial electrostatic dipole, as a function of position inside the structure, for a nitrobenzene molecule on a “medium” cluster (shown as inset). Arrows point to three special planes, each dividing the overall structure into two neutral subunits.

benzene derivatives given above. A plot of the dipole moment for the surface-adsorbed molecule, as a function of dipole in the gas phase, is given in Figure 2. The dependence is linear, as generally found for similar plots in experiments on mono-

layers,^{1,2} previous slab calculations,³⁹ and previous cluster calculations.²⁶ Using linear regression, slopes of 1.15, 1.48, and 1.55 are found for the “small”, “medium”, and “large” clusters, respectively. The larger than unity slope indicates a dipole

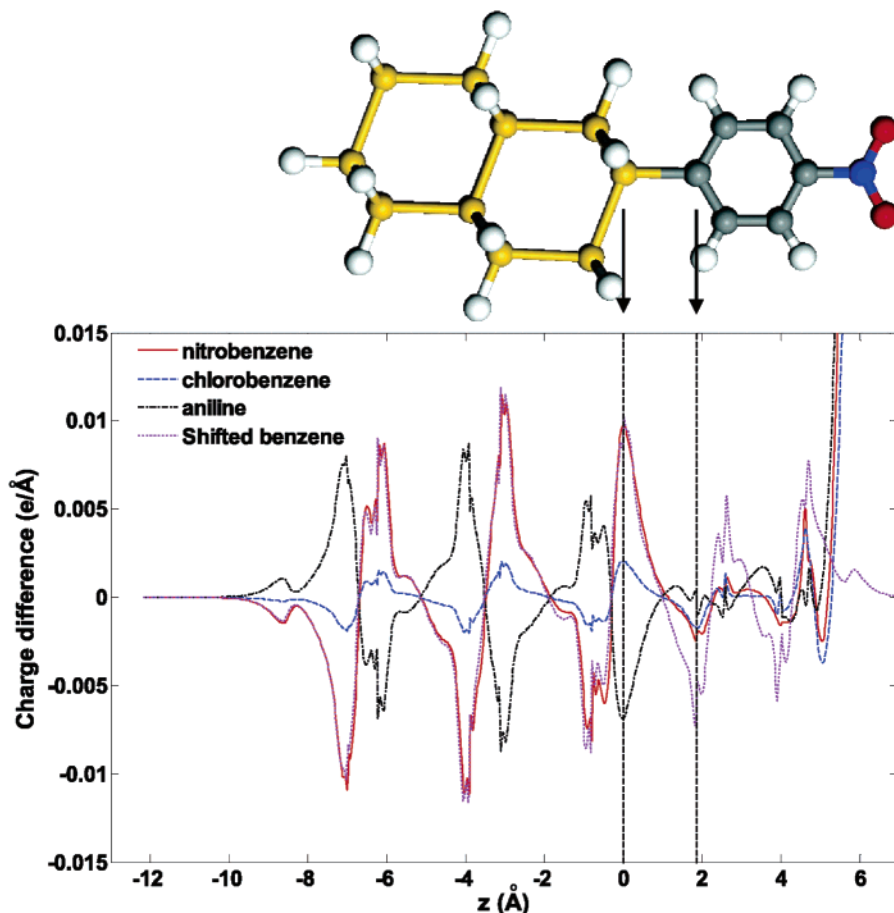


Figure 4. xy -averaged charge difference distributions, as defined in eq 2, as a function of vertical position, between the benzene-derivative-adsorbed and the benzene-adsorbed “medium” Si cluster, for nitrobenzene (solid line), chlorobenzene (dashed line), and aniline (dash-dotted line). The dashed lines at $z = 0$ and $z = 1.86$ Å denote the planes of the silicon and carbon atoms, respectively, that form the Si–C bond. Also shown (dotted line) is the charge-shifted benzene curve, as defined in eq 3, with a shift chosen so as to agree with the nitrobenzene charge difference curve.

enhancement, with the effect increasing with increasing cluster size. In the absence of geometry optimization of the cluster + molecule system, similar linear curves with slopes of 1.22, 1.4, and 1.48 are found. Clearly, geometry relaxation does not change the qualitative picture, an issue elaborated below.

To identify where the dipole enhancement is coming from, the *partial* dipole moment *distribution* along the z -axis was computed using the relation⁴⁷

$$P_z(z) = \int_z^\infty (z' - z) \rho(x, y, z') dx dy dz' \quad (1)$$

where z is the depth of an arbitrary plane inside the structure (with $z = 0$ taken as the plane of the silicon atom that is bonded to a carbon atom), P_z is the dipole between that plane and vacuum far from the cluster (from the molecule size), and $\rho(x, y, z)$ is the charge density (of both nuclei and electrons). Equation 1 has been previously recommended as superior (in terms of numerical stability) to a by-definition evaluation of partial dipoles.⁴⁷ It provides for values identical to those obtained from a by-definition calculation for all planes where the dipole is meaningful, i.e., those dividing the overall structure into neutral subunits. The positions of these planes are easily identified as that of extrema in the partial dipole dependence on z .⁴⁷

A typical partial dipole curve, for the case of nitrobenzene on a “medium” cluster, is shown in Figure 3. The continued

change in the extremal values of the curve shown in Figure 3 throughout the system indicates that the dipole is accumulated throughout and not just on the polar molecule. This indicates dipole *induction* across the substrate by the adsorbed molecule. Calculations similar to that shown in Figure 3 were performed for all molecules on both the “medium” and “large” clusters. For all physically meaningful special planes designated by arrows in Figure 3, plots similar to Figure 1, but with dependence of the *partial* dipole on the gas-phase dipole, were constructed. Just as in the case of Figure 1, all such plots yielded linear dependences. The results of the linear regression analysis are summarized in Table 1. The table shows that the partial dipole across the adsorbed molecule is only enhanced slightly and that most of the dipole enhancement is accumulated along the entire silicon cluster.

To interpret the dipole on the silicon cluster in terms of charge rearrangement, we studied the z -distribution of the xy -averaged *difference* between the valence charge density of the cluster with the functionalized benzene molecule, $\rho_F(x, y, z)$, and that with the benzene molecule itself, $\rho_B(x, y, z)$, in the form

$$\bar{\rho}_d(z) = \int_{-\infty}^{\infty} \int_{-\infty}^{\infty} (\rho_F(x, y, z) - \rho_B(x, y, z)) dx dy \quad (2)$$

Charge difference results for the “medium” cluster are shown in Figure 4. As expected chemically, there is a correlation

Table 1. Dipole Enhancement Factors Determined from Plots of Partial Dipoles as a Function of Gas-Phase Dipoles, with Partial Dipoles Assessed at Several Special Planes, Designated by Arrows in Figure 3

position of partial dipole	"medium" cluster	"large" cluster
at midplane of the silicon-carbon bond	1.14	1.13
at midplane of second and third silicon layers	1.33	1.34
at midplane of fourth and fifth silicon layers	1.45	1.45
entire cluster	1.5	1.54

between the sign and magnitude of the charge density difference and the extent of the electron donating/withdrawing nature of the functional group. As in the case of the dipole enhancement, the charge difference occurs mostly within the silicon cluster, with almost no charge difference in the benzene ring.

A detailed inspection of the charge density maps corresponding to different molecules establishes that, within the Si cluster, the charge difference, $\bar{\rho}_d(z)$, arises almost entirely from a *rigid shift* of the charge density. To show this quantitatively, we defined a *charge shifted xy-averaged* distribution, $\bar{\rho}_s(z)$, in the form

$$\bar{\rho}_s(z) = \int_{-\infty}^{\infty} \int_{-\infty}^{\infty} (\rho_B(x, y, z - z_0) - \rho_B(x, y, z)) dx dy \quad (3)$$

where for each functional group the rigid shift z_0 is chosen so as to minimize the residual difference between $\bar{\rho}_d(z)$ and $\bar{\rho}_s(z)$. z_0 values of ~ 0.05 , ~ 0.01 , and ~ -0.04 Å for nitrobenzene, chlorobenzene, and aniline, respectively, were found. In this way, the residual error, $|\bar{\rho}_s(z) - \bar{\rho}_d(z)|$, is substantially smaller than $\bar{\rho}_d(z)$ along the cluster and up to the middle of the Si-C bond, as can be seen in Figure 4 for the case of nitrobenzene. A similar level of agreement is obtained also for aniline and chlorobenzene (not shown in the figure for the sake of clarity). We define an overall "charge migration" across the plane of the carbon-bonded Si atom as

$$Q_d = \int_{-\infty}^0 \bar{\rho}_d(z') dz'$$

As shown in Table 2, Q_d can be a significant fraction of an electron, indicating that charge migration is a significant effect.

Importantly, the rigid valence charge shift is *not* simply due to a rigid shift of the nuclei: the average z -shifts in nuclear positions of the relaxed benzene-derivative-adsorbed clusters, with respect to the benzene-adsorbed clusters, were found to be ~ 0.02 , ~ 0.003 , and ~ -0.015 Å, for nitrobenzene, chlorobenzene, and aniline, respectively, i.e., less than half of the z_0 values given above. The dipole enhancement, then, is due to the difference between the close-to-rigid shift of the average electron cloud and the nuclear position distributions.

To correlate the electrostatic findings with molecular orbital trends, we consider the iso-density surfaces of the lowest unoccupied molecular orbital (LUMO) and highest occupied molecular orbital (HOMO) for the "medium" Si cluster with all four benzene derivatives studied here, shown in Figure 5. The LUMO of the clusters with aniline, benzene, and chlorobenzene; the HOMO of the nitrobenzene-adsorbed cluster; and certain portions of the HOMO of the cluster with benzene and chlorobenzene are localized on the cluster. Conversely, the

Table 2. Overall Charge Migration Index, Q_d , in Units of e , for the Three Benzene Derivatives

	"small" cluster	"medium" cluster	"large" cluster
aniline	0.04	0.18	0.37
chlorobenzene	-0.01	-0.06	-0.17
nitrobenzene	-0.05	-0.27	-0.62

LUMO of the cluster with nitrobenzene and the HOMO of the cluster with aniline are both localized on the molecule. A similar picture, albeit somewhat less sharply pronounced, holds for the "small" and "large" clusters as well.

The energy position of the HOMO and LUMO, for all cluster sizes and all benzene derivatives, is given in Figure 6, again as a function of the gas-phase dipole as in the case of Figure 2. We would expect that, per given benzene derivative, changing the cluster size would mostly shift the energy levels corresponding to molecular orbitals localized on the cluster. A significant distribution of energy level values per given molecule with different clusters can therefore serve as an indicator for localization of the orbital associated with this level on the cluster. When Figures 5 and 6 are compared, such a correlation is indeed observed. Changing the benzene derivative per given cluster size, we have already ascertained (cf. Figure 4) that the charge distribution difference occurs mainly inside the Si cluster. We therefore expect that energy levels corresponding to molecular orbitals localized inside the Si cluster would be more sensitive to the molecular dipole. Again, this is indeed observed in Figure 6. The LUMO energies of aniline, benzene, and chlorobenzene feature a linear dependence on the molecular gas-phase dipole moments, which is similar to that calculated previously for LUMO energies of polar dicarboxylic acids adsorbed on a GaAs cluster.²⁶ However, the LUMO energy of nitrobenzene does not share this linear dependence because it is localized on the molecule. The correlation between the HOMO orbitals and the gas-phase molecular dipole moments is not as distinct because, for, e.g., chlorobenzene, only a portion of the HOMO orbital is localized on the cluster.

2. A Phenomenological Classical Model. The valence charge density shifts discussed above strongly suggest the involvement of a dielectric response of the underlying substrate. To examine whether the electrostatic behavior can indeed be rationalized in such terms, and to offer a prediction for the behavior of larger clusters, we consider a highly simplified classical model of a point dipole above a uniform dielectric medium.

Consider a point dipole of magnitude P_0 , situated at a distance d above a uniform medium with a permittivity ϵ and perpendicular to the surface of the medium. The electric field in the dielectric region ($z < 0$) is then given by⁴⁹

$$E_z(r, \theta) = \frac{P_0}{4\pi\epsilon r^3} \cdot \frac{2\epsilon}{\epsilon + \epsilon_0} \cdot (3 \cos^2 \theta - 1) \quad (4)$$

where r , θ are the distance and angle (with respect to the z -axis) from the point dipole, and ϵ_0 is the vacuum permittivity.

(49) Jackson, J. D. *Classical Electrodynamics*, 3rd ed.; Wiley: New York, 1999; pp 145–156.

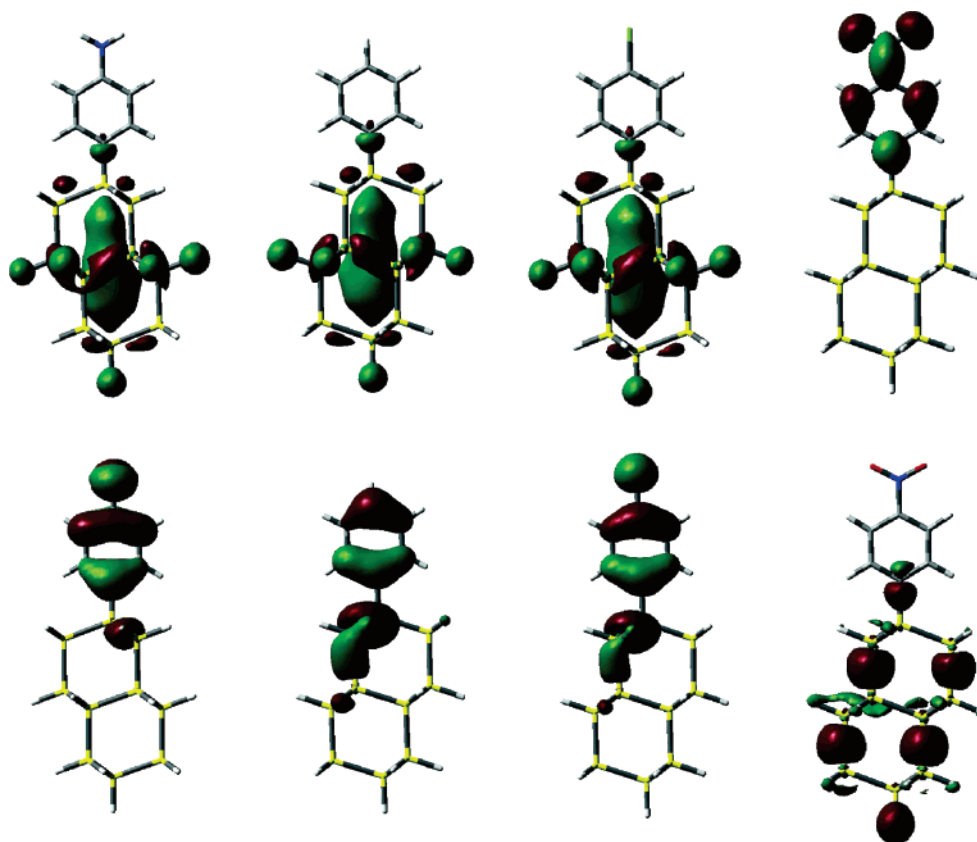


Figure 5. Iso-density surfaces of the LUMO (top) and HOMO (bottom) orbitals for the “medium” Si cluster adsorbed with different benzene derivatives. From left to right: aniline, benzene, chlorobenzene, and nitrobenzene.

ity. The induced polarization, P_z , is then (in Cartesian coordinates)

$$P_z = (\epsilon - \epsilon_0)E_z = \frac{P_0}{2\pi} \cdot \frac{\epsilon - \epsilon_0}{\epsilon + \epsilon_0} \cdot \left(\frac{3(d-z)^2}{(x^2 + y^2 + (d-z)^2)^{5/2}} - \frac{1}{(x^2 + y^2 + (d-z)^2)^{3/2}} \right) \quad (5)$$

Because P_z is, by definition, the dipole moment per unit volume, for an infinite surface the total dipole of the dielectric media is given by

$$P_\epsilon = \int_{-\infty}^0 dz \int_{-\infty}^{\infty} \int_{-\infty}^{\infty} P_z dx dy \quad (6)$$

Inserting eq 5 in eq 6 and performing the xy integration, we find that it vanishes for any value of z , so that $P_\epsilon = 0$. This seemingly surprising absence of overall induced polarization can be explained as follows. Defining the cylindrical coordinate $\rho = \sqrt{x^2 + y^2}$, we find using eq 5 that the integrand in eq 6 has positive values for $\rho \leq \sqrt{2}(d + |z|)$ and negative values elsewhere. This can also be rationalized by considering that the electric field lines of a point dipole must form closed loops. Thus, at an arbitrary z -plane, each electric field line must cross the plane twice, with the same sign as the dipole in the crossing point closer to it and the opposite sign in the farther crossing point. Importantly, we emphasize that neither the local electrostatic field nor the local dipole in the area under the point dipole vanish for an infinite surface—only the overall dipole does.

If we now model the cluster as a dielectric medium in the shape of a finite cylinder and the molecule as a point dipole, the total dipole is simply given by the sum of their dipoles, i.e.,

$$P = P_0 \left(1 + \frac{\epsilon - \epsilon_0}{\epsilon + \epsilon_0} \int_{-z_1}^0 dz \int_0^{\rho_1} \left(\frac{3(d-z)^2}{(\rho^2 + (d-z)^2)^{5/2}} - \frac{1}{(\rho^2 + (d-z)^2)^{3/2}} \right) \rho d\rho \right) \quad (7)$$

where z_1 and ρ_1 are the height and radius of the cylinder, respectively. Considering P as a function of ρ_1 , per given z_1 , we expect the total dipole to increase up to some critical cluster radius ρ_c and decrease beyond it, eventually tending toward zero. The actual value of the critical radius would depend strongly on the dipole–cluster distance d and on the cluster height z_1 .

Obviously the polar molecule is not a point dipole and the cluster is not a uniform medium. Thus, the naïve electrostatic model cannot be expected to provide quantitative predictions. Nevertheless, it does capture correctly the salient qualitative features of our quantum mechanical calculations. First, it explains the molecule-induced polarization of the Si cluster in terms of a dipole-induced dielectric response. Second, it predicts that, for finite clusters, a dipole enhancement would be observed because the molecular dipole is augmented by a net dipole over the cluster, in agreement with our calculations. Third, it predicts that, for small enough clusters, the dipole enhancement would increase with cluster size but that this increase would become smaller with increasing cluster size. This again agrees with our calculations, as the increase in dipole enhancement between the

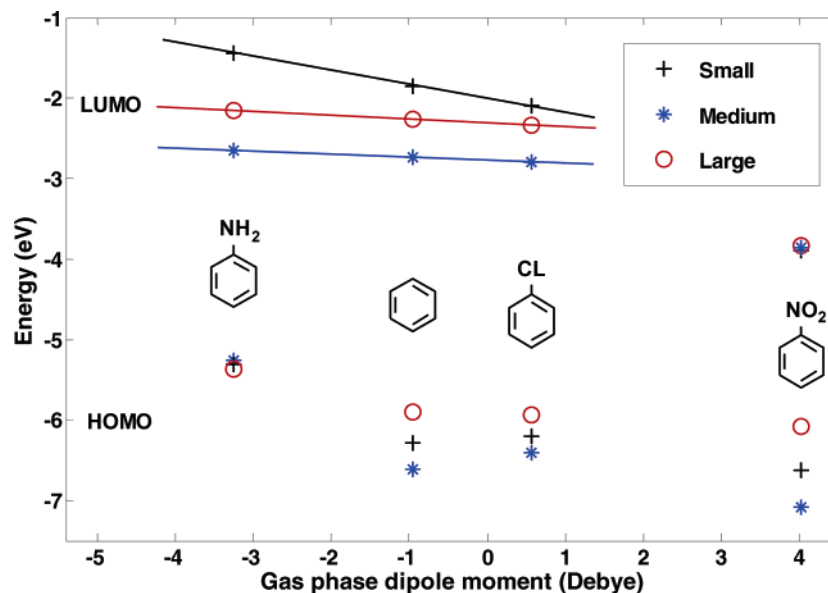


Figure 6. HOMO and LUMO energy levels of the four benzene derivatives adsorbed on the three cluster sizes of Figure 1, as a function of the dipole moment of the molecules in their gas phase. Straight lines are a guide to the eye.

“small” and “medium” clusters was much larger than that found between the “medium” and “large” clusters. We also note that the electrostatic model predicts that at cluster sizes beyond some critical radius (which apparently lies above the size of clusters reached by our quantum calculations) this dipole enhancement would decrease and eventually vanish.

3. Differences in Cluster and Slab Model Predictions.

Electrostatic trends that are completely different from those presented and rationalized above are obtained if a slab model is used. In fact, a previous plane wave slab calculation using the same substrate and molecules yielded diametrically opposite results.³⁹ A plot of the dipole moment for the surface-adsorbed molecule, as a function of the dipole for the gas-phase one, similar to that in Figure 2, exposed a dipole *reduction*, namely, a slope that is smaller than unity in the plot. This was rationalized electrostatically in terms of molecular polarization due to intermolecular dipole–dipole interactions. Moreover, the presence or absence of the underlying Si substrate did not change the picture significantly, indicating negligible substrate polarization or substrate-related dipole enhancement. To confirm that these significant changes are not due to the different basis sets used in the previous and present study, we repeated the “free-standing” molecular monolayer plane wave calculations of ref 39 with the localized orbital basis set used throughout this work. For 1ML and 0.5ML “coverage”, we obtained surface-adsorbed-molecule versus gas-phase-molecule dipole slopes of 0.56 and 0.74, respectively, as compared to 0.52 and 0.67 in the plane wave calculation.³⁹ While small numerical differences are apparent, the qualitative trend is exactly the same, clearly demonstrating that differences between the slab and cluster results are not basis set related.

The significant differences between slab and cluster calculations are a reflection of two completely different electrostatic phenomena dominating the behavior of adsorbed monolayers and single molecules, respectively. Because dipole depolarization is a direct consequence of intermolecular long-range interaction, it is rather obvious that it would be inherently missing when only one molecule is involved, i.e., would be found in slab calculations but not in cluster ones. The striking

difference in the substrate dielectric response between the cluster and slab calculations is, at first glance, much more surprising, given that the two systems model the same substrate. This is rationalized, however, by recalling that the behavior of the electrical potential inside the substrate is strikingly different in the two cases. For a single molecule, we expect a dielectric response to the significant electrostatic potential of a localized dipole, which scales as $\sim 1/r^2$. A significant dielectric response is indeed observed in our cluster calculations. However, for the monolayer we should expect a dielectric response to the potential outside a regular dipolar *array*. This potential decays *exponentially*, with a very short decay length of $L/2\pi$,^{47,50} where L is the intermolecular spacing. This dimension is typically shorter than the size of the benzene ring. Thus, the dipole-induced potential changes inside the substrate are negligible for a monolayer. They therefore elicit a negligible dielectric response, and indeed such a response is not observed in the slab calculations.

Further confirmation of this reasoning is obtained by examining a slab configuration with a partial coverage of 0.125 ML (namely, one adsorbed molecule per 16 surface Si atoms). Increasing the intermolecular spacing should yield a result intermediate between that of the isolated molecule and the complete monolayer. Indeed, integrating over an area similar to that of the “large” cluster,⁵¹ we found non-negligible charge migration in the slab, which was not observed for the 1 ML coverage. This again shows that the differences between cluster and slab calculations reflect a physical effect—different electrostatic properties—rather than a difference in numerical details.

The above discussion establishes that the properties of an adsorbed isolated polar molecule are *inherently* different from those of an adsorbed polar monolayer. The electrostatic differences imply that neither the molecular electron distribution nor the substrate one behave similarly in the two cases. For a

(50) Lennard-Jones, J. E.; Dent, M. *Trans. Faraday Soc.* **1928**, *24*, 92.

(51) Integration is performed over a limited lateral extent around the molecule for essentially the same reason as that in the discussion after eq 6: a null polarization would be obtained for an infinitely large surface. In a periodic representation this translates to a null polarization when integrating over the whole cell.

monolayer, the molecular polarization is very different from that of the gas phase, but the substrate is only weakly perturbed. For a single molecule, precisely the opposite statement holds! These differences can and generally will manifest themselves as differences in electronic structure, vibrational properties, reactivity, etc. This highlights the important role played by *long-range order*,⁵² in addition to local chemical properties, in tailoring surface chemistry via polar molecule adsorption¹³ and the importance of *cooperative* behavior in determining monolayer properties. Here, we focused on a single substrate, silicon, as a representative semiconductor. Naturally, metallic substrates may exhibit additional effects, and the magnitude of the response in insulators may differ from the one found here. Nevertheless, the cooperative electrostatic effect described here is of a general nature.

A corollary of the above conclusion is that cluster models involving a single molecule are inadequate for modeling adsorbed monolayers of polar molecules. In principle, one could construct models including several such molecules, at the cost of a significant increase in computational complexity. However, the dipole–dipole interaction is a highly long-range effect which would require unrealistically large clusters to capture correctly.

Importantly, the failure of the cluster model is *not* in contradiction to the above-discussed “near-sightedness principle”, because long-range electric fields are consistent with “near-sightedness” *only* if they are self-consistently added to the external potential.¹⁶ Indeed, the difficulties of cluster models in capturing electrostatic phenomena have been well-recognized in the literature in a different context, that of simulating highly ionic substrates, where a finite-sized cluster fails to capture the long-range Madelung potential. This is usually corrected for by “embedding” the cluster in a periodic array of classical positive and negative point charges (see, e.g., refs 53–55). The electrostatic potential is then included in the self-consistent solution of the Kohn–Sham equations, and “near-sightedness” is restored. For the present problem, one could similarly envision that a cluster could be embedded in a periodic array of classical point dipoles. This would surely suppress the electric field penetration into the cluster, as appropriate. However, for correctly capturing dipole–dipole induced depolarization, embedding in an array of *polarizable* point dipoles would be necessary. This is much more complicated. First, the embedding potential must be updated as part of the self-consistent loop. Second, a priori knowledge of the magnitude of both the gas-

phase dipole and the polarizability of the adsorbed species is required. Therefore, it is not clear whether this is a desirable approach in practice.

Just as a cluster model is a poor representation of a monolayer, a slab model is a poor representation of an isolated molecule on a surface, for essentially the same electrostatic reasons. In principle, a cluster model is suitable if the latter case is of interest. However, convergence with cluster size must be examined carefully. In our model system, the differences in dipole moment and charge reorganization between the “medium” and “large” clusters, though reasonably small, were definitely not negligible. This suggests that larger clusters yet may be necessary. As this may result in clusters too large to be computationally feasible, one may need to use different approaches for modeling the regions of the cluster that are far from the molecular adsorption site.

Conclusions

In conclusion, we have compared the electrostatic behavior of a single polar molecule adsorbed on a semiconducting substrate with that of an adsorbed polar monolayer. This was accomplished by density functional theory calculations with both cluster and slab models, using benzene derivatives adsorbed on the Si(111) surface as a representative test case. We found that cluster and slab models offer diametrically opposite descriptions of the surface electrostatic phenomena. In the nonperiodic cluster model, an overall dipole enhancement is found, caused mainly by a dipole-induced dielectric response that results in charge rearrangement within the substrate, with molecular polarization not being a significant effect. Conversely, in the periodic slab model an overall depolarization effect is found, caused by dipole–dipole interactions that polarize the molecular electron cloud, and the substrate plays a negligible role due to electric field suppression outside the monolayer. These differences may lead to surface chemical properties that are a strong function of monolayer coverage and order, establishing the crucial role of long-range, cooperative behavior, in addition to local chemical properties, in tailoring surface chemistry via polar molecule adsorption.

Acknowledgment. We wish to thank Ron Naaman, David Cahen, Lior Segev (Weizmann Inst.), and Abraham Nitzan (Tel Aviv U.) for illuminating discussions. L.K. acknowledges financial support from the Israel Science Foundation (“Bikura”), the Gerhard Schmidt Minerva Center for Supra-Molecular Architecture, the “Phoremot” European Network of Excellence, and the Delta Career development chair.

Supporting Information Available: Full citation for ref 40. This material is available free of charge via the Internet at <http://pubs.acs.org>.

JA068417D

(52) Here, we discussed an ideally ordered monolayer on an ideally ordered substrate. Deviations from the perfectly ordered monolayer/substrate discussed here (as in, e.g., rough or stepped surfaces) may allow for some field penetration into the substrate. This will be discussed in detail elsewhere.

(53) Sushko, P. V.; Shluger, A. L.; Baetzold, R. C.; Catlow, C. R. A. *J. Phys.: Condens. Matter* **2000**, *12*, 8257.

(54) Jug, K.; Bredow, T. *J. Comput. Chem.* **2004**, *25*, 1551.

(55) Sauer, J. *Chem. Rev.* **1989**, *89*, 199.